

# Journal of Biomedical Optics

[SPIDigitalLibrary.org/jbo](http://SPIDigitalLibrary.org/jbo)

## ***Ex vivo* comparison of the tissue effects of six laser wavelengths for potential use in laser supported partial nephrectomy**

Wael Y. Khoder  
Katja Zilinberg  
Raphaella Waidelich  
Christian G. Stief  
Armin J. Becker  
Thomas Pangratz  
Georg Hennig  
Ronald Sroka

# Ex vivo comparison of the tissue effects of six laser wavelengths for potential use in laser supported partial nephrectomy

Wael Y. Khoder,<sup>a</sup> Katja Zilinberg,<sup>a</sup> Raphaela Waidelich,<sup>a</sup> Christian G. Stief,<sup>a</sup> Armin J. Becker,<sup>a</sup> Thomas Pangratz,<sup>b</sup> Georg Hennig,<sup>b</sup> and Ronald Sroka<sup>b</sup>

<sup>a</sup>University Hospital Munich–Grosshadern, Department of Urology, Ludwig-Maximilians-University Munich, Marchioninistrasse 15, 81377 Munich, Germany

<sup>b</sup>University Hospital, Laser-Forschungslabor, LIFE-Centre, Ludwig-Maximilians-University Munich, Marchioninistrasse 23, 81377 Munich, Germany

**Abstract.** Laparoscopic/robotic partial nephrectomy (LPN) is increasingly considered for small renal tumors (RT). This demands new compatible surgical tools for RT-resection, such as lasers, to optimize cutting and coagulation. This work aims to characterize *ex vivo* handling requirements for six medically approved laser devices emitting different light wavelengths (940, 1064, 1318, 1470, 1940, and 2010 nm) amenable for LPN. Incisions were made by laser fibers driven by a computer-controlled stepping motor allowing precise linear movement with a preset velocity at a fixed fiber-tip distance to tissue. Optical parameters were measured on 200  $\mu\text{m}$  tissue slices. Cutting quality depended on power output, fiber velocity and fiber-tip distance to tissue. Contact manner is suitable for cutting while a noncontact manner (5 mm distance) induces coagulation. Ablation threshold differs for each wavelength. Ablation depth is proportional to power output (within limit) while axial and superficial coagulation remains mostly constant. Increased fiber velocity compromises the coagulation quality. Optical parameters of porcine kidney tissue demonstrate that renal absorption coefficient follows water absorption in the 2  $\mu\text{m}$  region while for other spectral regions (900 to 1500 and 1  $\mu\text{m}$ ) the tissue effects are influenced by other chromophores and scattering. Tissue color changes demonstrate dependencies on irradiance, scan velocity, and wavelength. Current results clearly demonstrate that surgeons considering laser-assisted RT excisions should be aware of the mentioned technical parameters (power output, fiber velocity and fiber-tip tissue-distance) rather than wavelength only. © 2012 Society of Photo-Optical Instrumentation Engineers (SPIE). [DOI: [10.1117/1.JBO.17.6.068005](https://doi.org/10.1117/1.JBO.17.6.068005)]

Keywords: laser supported partial nephrectomy; lasers in urology; optical properties of renal tissue.

Paper 12067 received Feb. 1, 2012; revised manuscript received Apr. 22, 2012; accepted for publication May 8, 2012; published online Jun. 12, 2012.

## 1 Introduction

Owing to the widespread use of screening abdominal ultrasound and computer tomography (CT), the number of incidentally diagnosed small renal tumours (RT) has been increasing.<sup>1</sup> Surgical excision is currently considered the only curative treatment for RT. Thus nephron sparing surgery (NSS) is increasingly indicated, while radical nephrectomy is increasingly considered an overtreatment.<sup>2</sup>

The primary goal of NSS is to excise RT with a safety margin of normal renal parenchyma. Laparoscopic (LPN) and robotic-assisted (RPN) partial nephrectomy are increasingly indicated due to minimal invasive advantage and superior postoperative recovery compared to open surgery.<sup>3</sup> Several reports document comparable perioperative, functional and long-term oncological outcomes of LPN/RPN with open surgery.<sup>4</sup>

While disadvantages of LPN have been decreasing over the last decade, recent expansion of its indications opened a demand for compatible surgical tools to allow precise and fast RT-excision with easy manipulations, fewer side effects and excellent hemostasis for clear laparoscopic vision.<sup>5</sup>

Energy-based technologies like monopolar or bipolar cautery, argon beam coagulation and radio frequency tools are used for adequate hemostasis during NSS.<sup>6</sup> While experimental reports have evaluated laser application with/without hilar clamping,<sup>6–11</sup> adequate laser adjustments, intraoperative maneuvers and fiber-tissue distance suitable for LPN still have to be defined. For this purpose six medically approved laser devices emitting light at different wavelengths were compared in an *ex-vivo* investigation as an effort to establish a safe comparable technique of laser-supported laparoscopic partial nephrectomy (LLPN).

## 2 Materials and Methods

### 2.1 Tissue Model

Laser cutting efficiency experiments were performed on renal surfaces devoid of surrounding renal fat leaving the renal capsule completely intact mimicking the clinical situation. Fresh porcine kidneys ( $n = 50$ ) were rinsed with saline through their arteries until blood-free solution was released from the renal vein before experiments. Thus reproducible tissue conditions are obtained.

Address all correspondence to: W. Khoder, Department of Urology, Großhadern University Hospital, LMU, Marchioninstr. 15, 81377 Munich, Germany. Tel: +49 (0)89 ext 70950; Fax: +49 (0)89 7095 8735; E-mail: [wael.khoder@med.uni-muenchen.de](mailto:wael.khoder@med.uni-muenchen.de)

**Table 1** Physical properties of the six different laser systems examined in current study for potential use in laser-supported partial nephrectomy. All except one laser (Costume made property: DL1470 nm) are medically certified.

| Laser systems                                 | Laser type    | Wavelength (nm) | Power on console (W) | Fiber core diameters ( $\mu\text{m}$ )/NA |
|---|---------------|-----------------|----------------------|---|
| MediLas D, DornierMedTec (Germering, Germany) | Diode         | 940             | 10–60                | 600/365/0.37                              |
| Fibertom, DornierMedTec (Germering, Germany)  | Nd:YAG        | 1064            | 10–100               | 600/365/0.2                               |
| Eraser, Rolle & Rolle (Salzburg, Austria)     | Diode         | 1318            | 10–100               | 600/365/0.37                              |
| Costume made prototype                        | Diode         | 1470            | 10–40                | 600/365/0.37                              |
| Vela XL, StarMedTec (Starnberg, Germany)      | Thulium-fiber | 1940            | 10–120               | 600/365/0.2                               |
| Cyber Tm 150, Quanta (Milano, Italy)          | Tm:YAG        | 2010            | 10–150               | 600/365/0.2                               |

## 2.2 Laser Equipment

Six medical laser systems emitting light at wavelengths from  $\lambda = 940$  to 2010 nm in continuous-mode were investigated. The laser beam was transmitted through quartz-glass fibers at core diameter of 600 and 365  $\mu\text{m}$  for each wavelength and different NA of 0.2 and 0.37 (Table 1).

## 3 Laser Cut/Coagulation Qualities (Clinical Mimicking)

### 3.1 Experimental Setup

In Fig. 1 the experimental setup with kidneys positioned on a glass basin is shown. Laser fiber was fixed to a height-adjustable arm, which could be moved along the specimens by a computer-controlled stepping motor. This unit allows for precise linear fiber movement with a preset defined velocity ( $v_{\text{fiber}}$ ) at fixed fiber-tip distance to tissue surface producing 4 cm incisions. Experiments were performed in air with smoke suction mimicking *in-vivo* laparoscopic conditions.

### 3.2 Experiments and Measurements

Cutting quality of each laser system was estimated for each laser power output, [ $v_{\text{fiber}}$ ] and distance between fiber tip and tissue. First set was 1 mm/s fiber velocity in contact manner (0 mm distance to tissue), mimicking tissue-contact mode with slow movement clinically. Power output was increased in increments of 10 W, beginning with 10 W to highest possible console values. The same experiments were repeated for 5 mm distance.

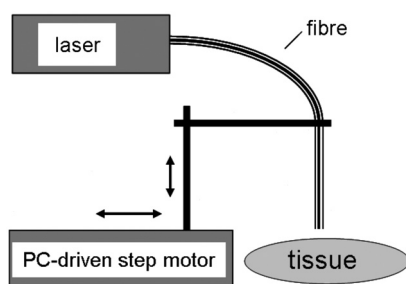


**Fig. 1** Experimental setup for evaluation of laser light application in respect to fiber velocity and distance to tissues. This setup mimics the potential clinical situations.

Next, [ $v_{\text{fiber}}$ ] was changed to 5 mm/s and then to 10 mm/s. These parameter combinations mimic the potential different clinical situations.

Three linear incisions were performed on different kidneys for each set of parameters. Measurements (ablation depth, ablation width, axial and superficial lateral coagulation depths and color) were performed at three locations along each incision on the surface and on sagittal sections by means of venier calipers (Fig. 2). Surface irregularities were avoided. Ablation was defined as complete tissue loss. The coagulation zone was verified as the white-colored tissue surrounding the ablation area by visual appearance. Carbonization was classified as minor (brown-colored tissue) and major (black) on the remaining surface. Examined specimens and sagittal sections were documented photographically [Fig. 2(b)].

### 3.3 Evaluation

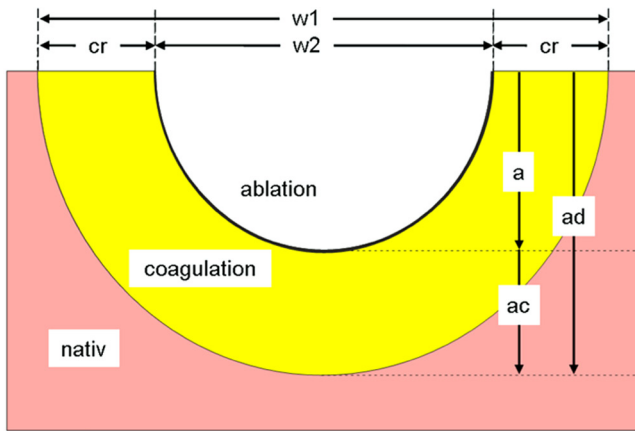
The mean and standard deviation of all measured raw data values (Fig. 2) were calculated and plotted in dependency to power output. Statistics [*t*-test, one-way Anova, significances ( $p < 0.05$ )] were performed (SigmaPlot 11.0, JandlScientific). For comparison purposes, the applied linear irradiance dose (ALID) [ $\text{J}/\text{cm}$ ] = (Output power)/velocity [ $\text{W}/(\text{cm}/\text{s})$ ] was calculated.<sup>12</sup> The appearance of subjective surface colors were classified and correlated to the laser output power and listed for comparison according to scan velocity and wavelength [Fig. 2(b)].

## 4 Optical Properties of Renal Tissue

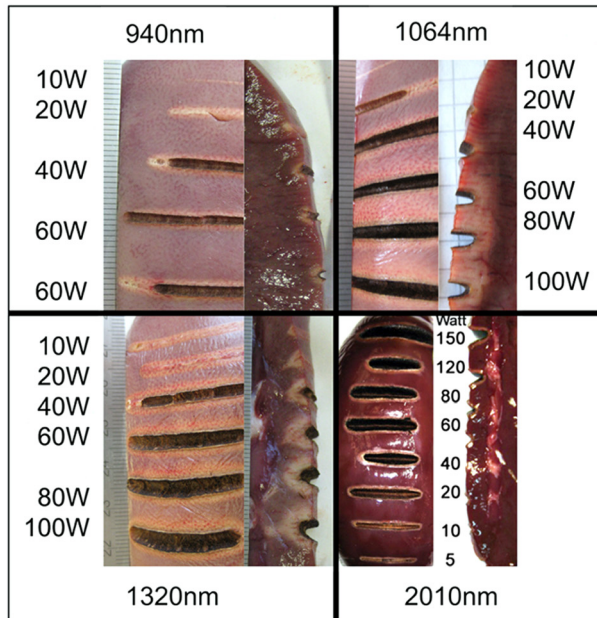
Optical properties of kidney tissue in this spectral region were measured to provide the rationales for ablation/coagulation effects during laser-light tissue interactions.

### 4.1 Experimental Setup

Optical parameters were measured on tissue slices squeezed between two slides with a 200  $\mu\text{m}$  spacer to define thickness and geometry. Each collimated laser beam was directed through the tissue samples to measure its optical transmission through the detector (AC25HD, Scientech®) positioned distant to the sample. An additional aperture in the optical detection pathway served for detection of only forward scattered and nonscattered photons (Fig. 3).



(a)



(b)

**Fig. 2** Evaluation of laser induced tissue effects. (a) Schematic cut through tissue showing definitions of tissue states and measured values defined as: w1: superficial affected diameter; w2: superficial diameter of ablation; a: axial ablation depth; ad: total affected axial depth. Based upon these raw data the lateral coagulation rim [ $Cr = w1 - w2/2$ ] and [ $ac = ad - a$ ] were calculated for further evaluation. (b) Tissue samples (superficial view and saggital cuts) with laser-induced lesions in kidneys performed by different wavelengths and laser powers. Note the color changes and the carbonized surface with underlying whitish coagulation according to the applied laser power. All experiments are performed in contact mode and scan-velocity of 1 mm/s.

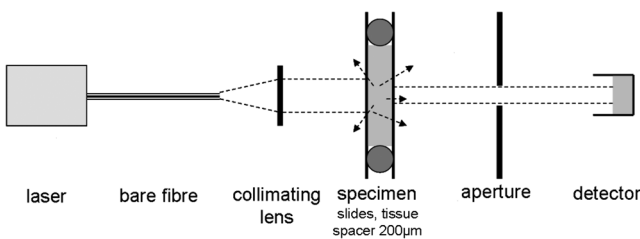


**Fig. 3** Experimental setup for measuring optical transmission through slices of porcine kidney tissues.

## 4.2 Experiments and Measurements

Measurements were performed on five different kidney samples ( $n = 14$  positions) for each wavelength. Light intensity was reduced to avoid tissue thermal effects. Correction measurements were performed prior to each tissue measurement. Undisturbed laser-light intensity was measured within empty setup prior and immediately after each sample measurement to detect any intensity fluctuations. The mean of the two measurements was taken as incident intensity ( $I_0$ ). Afterward, the intensity transmitted through 200  $\mu\text{m}$ -thick water in between two slides ( $I_{\text{water}}$ ) was measured to correct for light slide transmission/reflection. Last, the transmitted tissue intensity ( $I_{\text{kidney}}$ ) was measured.

## 4.3 Evaluation

The total attenuation coefficient ( $\mu_t$ ) of samples (water, kidney) was calculated according to the Lambert-Beer-law.

$$I_{\text{sample}} = (I_0 - I_{\text{reflex}}) \cong \exp[-\mu_t(\text{sample}) \cong d]. \quad (1)$$

Water measurements were used to calculate the unknown reflected intensity  $I_{\text{reflex}}$ , estimating the intensity losses at sample holder surfaces for water and kidney are equal (similar refractive index). The correction for water absorption was performed using Eq. (2). As the absorption of water  $\mu_{a(\text{water})}$  is known<sup>13,14</sup> and assuming  $\mu_{t(\text{water})} = \mu_{a(\text{water})}$ , the value of  $I_{\text{reflex}}$  can be calculated by means of Eq. (1) as follows:

$$I_{\text{reflex}} = -I_{\text{water}} / \exp[-\mu_{a(\text{water})} \cong d] + I_0 \quad (2)$$

[ $\mu_{a(\text{water})}$  from Refs. 13 and 14,  $d = 200 \mu\text{m}$ ].

Using  $I_{\text{reflex}}$  to correct for light reflexes,  $\mu_{t(\text{kidney})}$  can be calculated.

$$\mu_{t(\text{kidney})} = -\log[I_{\text{kidney}} / (I_0 - I_{\text{reflex}})] / d. \quad (3)$$

The mean and standard deviation of  $\mu_{t(\text{kidney})}$  were plotted for each wavelength together with the water absorption.<sup>13,14</sup> In Table 2 the wavelengths' specific attenuation  $\mu_{t(\text{kidney})}$  were listed compared to  $\mu_{a(\text{water})}$ <sup>13,14</sup> and the difference  $\mu_{t(\text{kidney})} - \mu_{a(\text{water})}$ , which indicates the sum of light losses only due to scattering and absorption by kidney chromophores [ $\mu_{s(\text{kidney})} + \mu_{a(\text{ch-kidney})}$ ].

## 5 Results

Generally, the wavelength cutting quality differed in respect to power output,  $v_{(\text{fiber})}$  and distance to tissue. Smooth cuts and ablation and coagulation margins were macroscopically obvious.

Figure 4 shows the results in relation to power output for the six wavelengths using the same reproducible parameters (tissue contact, 600  $\mu\text{m}$ -fiber,  $v_{(\text{fiber})} = 1 \text{ mm/s}$ ). Continuous and nearly linear increase of ablation depth was observed with increasing power output [Fig. 4(a)]. Noninfrared (NIR)-lasers ( $\lambda = 940 \text{ nm}$ , 1064 nm and 1318 nm) and infrared (IR) lasers ( $\lambda = 1470, 1940, \text{ and } 2010 \text{ nm}$ ) induced obviously different tissue effects. NIR lasers showed threshold power output between 10 and 20 W, at which the IR group already resulted in ablation depth of 1 to 2 mm. IR wavelengths produced a significantly

**Table 2** Optical correlation of the tissue surface appearance (colors) to laser output to different fiber velocities during laser-induced cutting experiments using 2010 nm in continuous wave and contact mode.

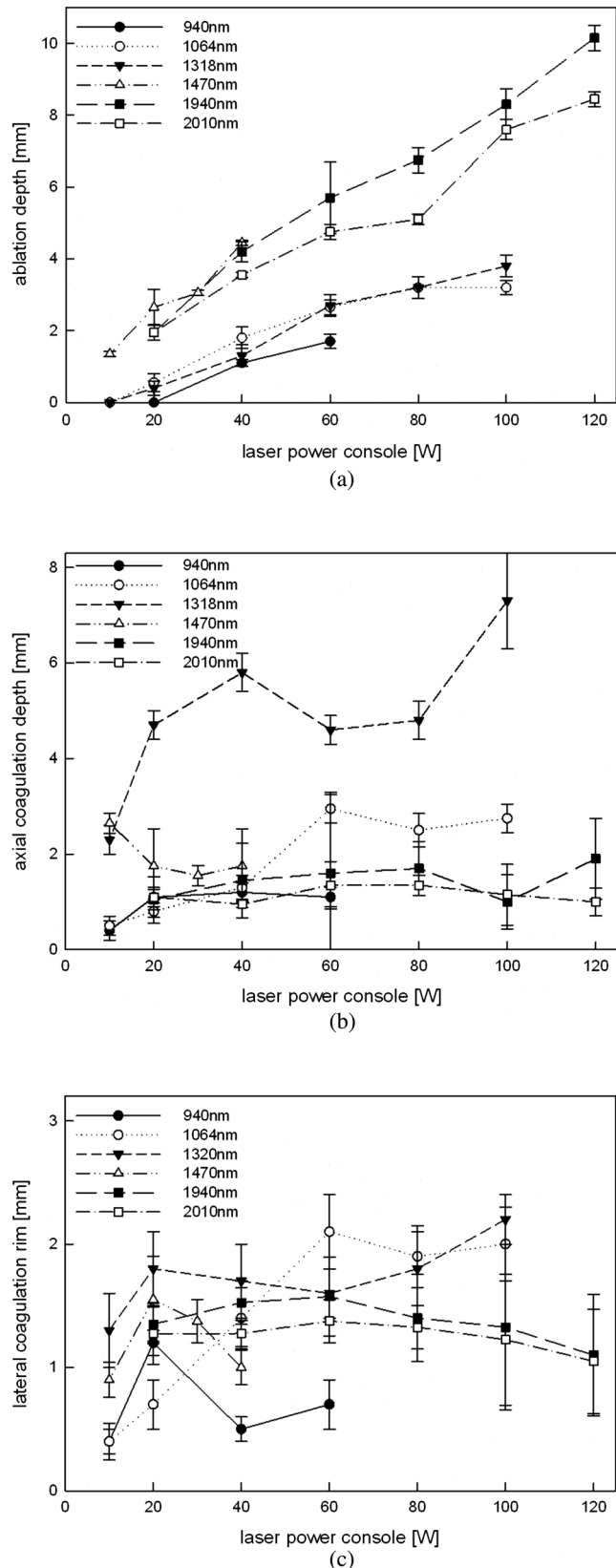
| 2010 nm, cw, Contact-mode | Correlation of apparent tissue surface color to laser power |             |                     |
|---------------------------|---|-------------|---------------------|
| Scan-velocity             | Whitish-coagulation   | Brown       | Black-carbonization |
| 1 mm/s                    | 5 W   | 10 to 20 W  | ≥40 W               |
| 5 mm/s                    | 5 to 20 W   | 40 to 60 W  | ≥80 W               |
| 10 mm/s                   | 5 to 40 W   | 60 to 120 W | ≥150                |

deeper ablation crater ( $p < 0.05$ ) compared to NIR wavelengths, whereas no significance was found within each group. As shown in Fig. 4(b), the axial coagulation showed insignificant differences dependent upon power output for all wavelengths, except for 1318 nm ( $p < 0.05$ ). Interestingly, axial coagulation was reduced when power outputs of  $\leq 20$  W were applied. The same effect was seen for superficial coagulation [Fig. 4(c)] with values between 0.5 and 2.5 mm without any significance between wavelengths. After reaching a maximum, the values remain approximately constant for each wavelength.

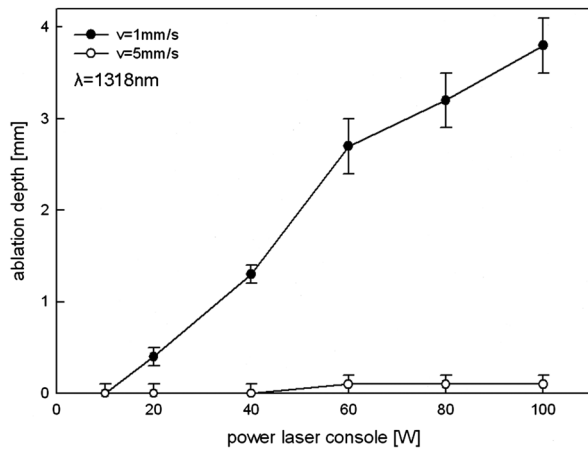
The influence of fiber velocity on the ablation depth in contact mode is shown in Fig. 5. In the case of 1318 nm [Fig. 5(a)], ablation occurs on exceeding an ablation threshold of about 20 W for  $v_{(fiber)} = 1$  mm/s (ALID = 200 J/cm). Contrary, at 5 mm/s no ablation could be measured even on reaching power outputs of 100 W at the same ALID. In the case of 1940 nm, a significant reduction in ablation depth with increased  $v_{(fiber)}$  could be shown [Fig. 5(b)]. Similar ablation depth occurred at equal ALID-values of 200 J/cm. Axial coagulation remained constant (0.3 to 2.0 mm) with increasing power output. As a third example in Fig. 5(c) the results using 2010 nm light showed not only significant reduction of ablation depth but also different ablation thresholds, such as  $< 5$  W, 5 to 10 W, 40 to 60 W when  $v_{(fiber)}$  was increased from 1 mm/s to 5 to 10 mm/s, respectively. Interpolation of a comparable ALID = (200  $\cong$  50) J/cm showed similar ablation depths. While axial coagulation is reduced with increasing  $v_{(fiber)}$ , superficial coagulation was found constant.

Figure 6 shows changes in ablation in respect to fiber-tip tissue distance at the same  $v_{(fiber)}$ . Using 1470 nm wavelength resulted in significant reduction in ablation depth when increasing tissue distance from 0 to 5 mm [Fig. 6(a)] accompanied by an increase of the ablation threshold value from  $< 10$  to 20 W. In case of 2010 nm light application [Fig. 6(b)] a slight insignificant reduction in ablation depth (filled markings) and a significant reduction in axial coagulation (open markings) were found, when increasing the distance.

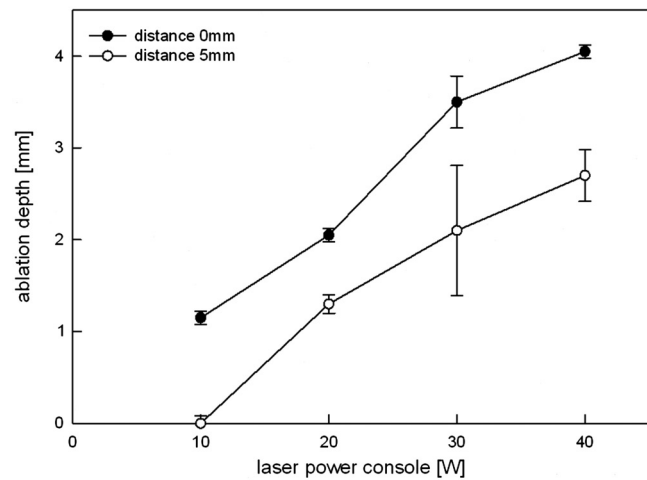
Efficient cutting could be obtained in fiber contact to tissue. A comparison of the ablation capacity of fibers with different core-diameters under same conditions was performed. Figure 7 shows the example of 1470 nm that ablation depth depends on power output without any significant difference between fibers with 365  $\mu$ m versus 600  $\mu$ m core diameters. This was observed for each wavelength. Further, no differences in coagulation size, either axial or superficial, was found.



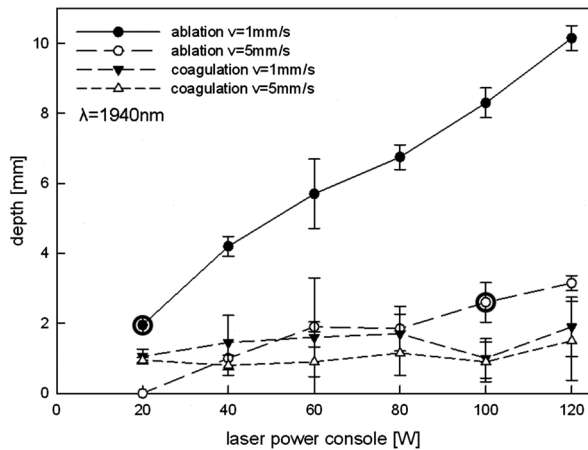
**Fig. 4** Illustration of laser-induced tissue effects in ex vivo kidney model. Laser light was applied in contact mode, fiber velocity = 1 mm/s, 600  $\mu$ m fiber-core diameter. (a) Ablation depth show significant differences between IR-group and NIR-group ( $p < 0.05$ ). (b) Axial coagulation depth show no significance ( $p > 0.05$ ) except 1318 nm. (c) Superficial lateral coagulation rim have no relation to wavelength.



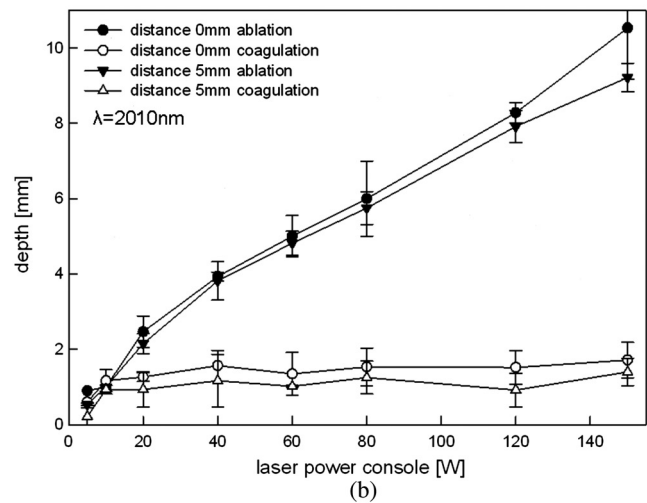
(a)



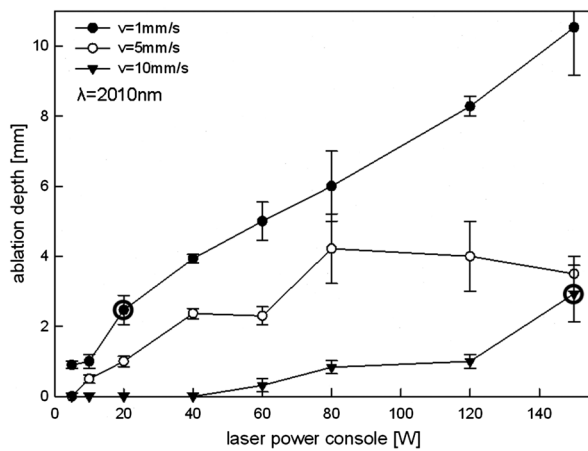
(a)



(b)



(b)



(c)

**Fig. 5** Illustration of laser-induced tissue effects in *ex vivo* kidney model according to different fiber velocities in contact mode, fiber core diameter  $600\ \mu\text{m}$ . (a) Experiment for 1318 nm laser light showing significant reduction of ablation depth with increasing fiber velocity ( $p < 0.05$ ). (b) Experiment for 1940 nm laser light. Significant ( $p < 0.05$ ) reduction of ablation depth according to fiber velocity with shift of ablation threshold from  $<20\ \text{W}$  to 20 to 40 W. Approximately the same ALID-200 J/cm show similar ablation depth. Axial coagulation depth is not significantly different ( $p > 0.05$ ). (c) Experiment for 2010 nm laser light. Significant ( $p < 0.05$ ) reduction of ablation depth according to fiber velocity. Threshold shift from  $<5\ \text{W}$ ,  $<10$  to  $<60\ \text{W}$ . Approximately the same ALID- $(200 \pm 50)$  J/cm show similar ablation depth.

**Fig. 6** Illustration of laser-induced tissue effects in *ex vivo* kidney model according to different distances between fiber tip and tissue surface. (a) Experiment for 1470 nm laser light, velocity = 1 mm/s. Significant reduction of ablation depth by about 1 mm and ablation threshold shift according to distance increase from 0 to 5 mm ( $p < 0.05$ ). (b) Experiment for 2010 nm laser light, velocity = 1 mm/s. No significant ( $p > 0.05$ ) reduction of ablation depth by less than 1 mm and minor shift of ablation threshold according to distance increase from 0 to 5 mm. Also a reduction in the coagulation by about 0.5 mm could be observed without significance ( $p > 0.05$ ).

Thorough examination of the tissue pictures, deduced tissue surface color changes from whitish (coagulation) over brown to black (minor to major carbonization) with increasing the laser power in an approximately stepwise manner as shown in Fig. 2(b). Table 2 lists these changes in respect to fiber velocity results for the 2010 nm experiment and shows the shifted appearance of the color changes, which is due to the different ALID applied. Comparing the apparent color changes (whitish, brown or black surface color) according to the used wavelength under comparable experimental conditions (contact mode and scan velocity of 1 mm/s) shows a possible wavelength dependence to the onset of color change as listed in Table 3.

The calculated optical parameters of porcine kidney tissue are listed in Table 4 and Fig. 8. Both demonstrate that  $\mu_{t(\text{kidney})}$  follows  $\mu_{t(\text{water})}$  especially in the  $2\ \mu\text{m}$  region where water dominates light attenuation. In the 1300 to 1500 nm region, the curve of light attenuation in water is retraced by

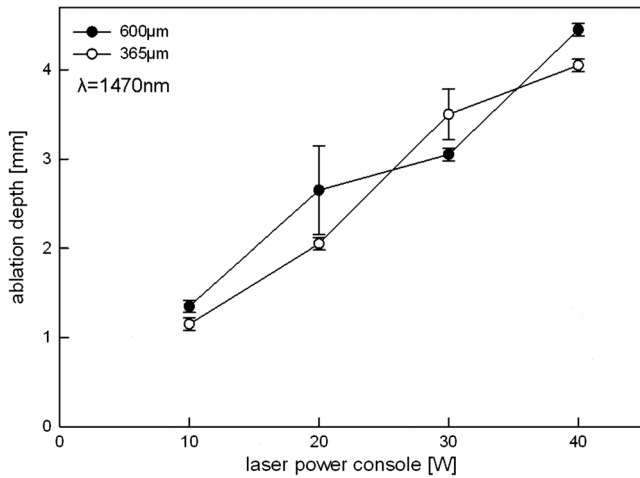


**Fig. 7** Laser tissue effects ( $\lambda = 1470$  nm, contact mode, velocity = 1 mm/s) in relation to different fiber core diameters show no significant difference ( $p > 0.05$ ) either in ablation depth (data shown) or in axial coagulation depth or in lateral coagulation rim (data not shown) because of exceeding ablation threshold.

the measured values although there is superposition with other absorber chromophores as well as scattering attenuations effect involved. The 1  $\mu$ m region is dominated by further absorbing and scattering components.

### 6 Discussion

Current LPN techniques are still in need for further refinements. Many aspects make these techniques challenging. Intraoperative hemostasis aids not only to avoid excessive blood loss but also to allow precise tumor excision, surgical closure of the collecting system and re-approximation of parenchyma-defect in a bloodless field.<sup>6,15</sup> This often necessitates hilar clamping, which adds time constraints on the surgeon.<sup>16</sup> Warm ischemia (WI) should be better avoided or kept at a minimum ( $\leq 20$  min.) to avoid kidney damage as WI is the most important factor governing the return of renal function postoperatively.<sup>17</sup> Haemostasis after tumor excision is important to prevent

**Table 3** Subjective correlation of the appearance of tissue surface colors to laser output and different wavelengths used for laser-induced cutting experiments by means of continuous wave, fiber velocity of 1 mm/s and contact mode.

| Contact-mode<br>v=1 mm/s | Correlation of appeared tissue surface color to laser power |            |                     |
|--------------------------|---|------------|---------------------|
|                          | Whitish-coagulation   | Brown      | Black-carbonization |
| 940                      | 10 to 20 W  |            | $\geq 40$ W         |
| 1064                     | 10 W  | 20 W       | $\geq 40$ W         |
| 1318                     | 10 to 20 W  | 40 W       | $\geq 60$ W         |
| 1470                     | 10 to 20 W  | 30 W       | 40 W                |
| 1940                     | 5 W   | 10 to 20 W | $\geq 40$ W         |
| 2010                     | 5 W   | 10 to 20 W | $\geq 40$ W         |

**Table 4** Optical properties of porcine kidney tissue for five laser wavelengths (1064 nm not measured).  $\mu_{t(kidney)}$ : attenuation coefficient of kidney tissue,  $\mu_{a(H_2O)}$ : absorption coefficient of water,<sup>13,14</sup>  $\mu_{s(kidney)} + \mu_{a(ch-kidney)}$ : scattering and absorption by kidney chromophores.

| Wavelength (nm) | $\mu_{t(kidney)}$ (1/mm) | $\mu_{a(H_2O)}$ (1/mm) | $\mu_{s(kidney)} + \mu_{a(ch-kidney)}$ (1/mm) |
|-----------------|--------------------------|------------------------|---|
| 940             | 11.1 $\pm$ 1.0           | 0.001                  | 11.1  |
| 1318            | 6.5 $\pm$ 0.6            | 0.2                    | 6.3   |
| 1470            | 8.0 $\pm$ 1.0            | 2.8                    | 5.2   |
| 1940            | 13.8 $\pm$ 1.2           | 12.6                   | 1.2   |
| 2010            | 9.8 $\pm$ 0.7            | 6.2                    | 3.6   |

postoperative bleeding. Saving the collecting system together with minimal parenchyma damage are also main principles.<sup>18</sup> However, the reported intraoperative complication rate was 5.5%.<sup>19</sup> Further, independently from LPN technique, the instrumentation for tumor excision and parenchyma reconstruction should be easy to handle to avoid additional challenges. Therefore, a new modality of RT resection is still required.

Laser technologies are established standard modalities for some urological applications e.g., BPH surgery<sup>20</sup> and lithotripsy,<sup>21</sup> while still searching for new applications.<sup>22</sup> Laser applications for NSS have been investigated in animal models<sup>6-11,23-26</sup> and clinical trials<sup>5,27-29</sup> None of these efforts reached widespread use for NSS. The aim of the current work was to mimic the required intraoperative maneuvers for different lasers transmitted through end-firing laser-fibers for resection of renal tissue as a primary step in establishing feasible LLPN technique and to compare the capability characteristics of different wavelengths.

While urological laser vaporisation studies are consistent,<sup>20</sup> investigations on comparisons of laser cutting quality and coagulation depth are not available. According to the tissue optical

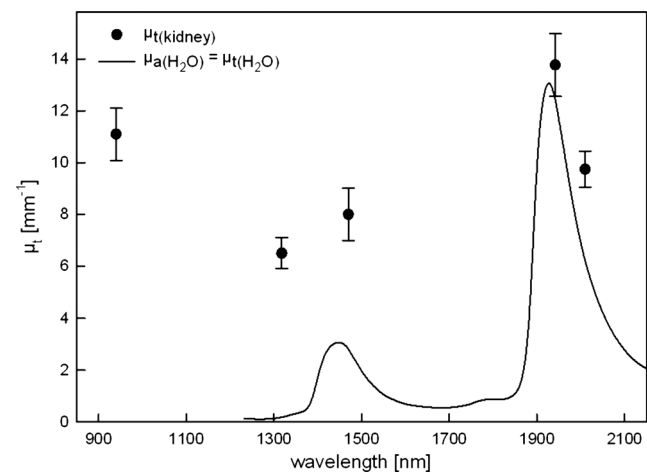


**Fig. 8** Kidney optical attenuation coefficient in comparison to water absorption coefficient<sup>13,14</sup> in the spectral region of 900 to 2150 nm. Values are also listed in Table 4.

parameters, every wavelength may show its own characteristics in cutting/coagulation. Based on the presented  $\mu_{t(\text{kidney})}$ -values, different absorber concentrations in relation to tissue water affect the wavelength dependent tissues absorption/scattering processes, which is the rationale of the observed differences in ablation/coagulation capacity of each tested laser-wavelength. Current study included laser wavelengths of clinical interest. The 532 and 810 nm were not included in the study as they are mainly used for prostate vaporization in underwater setup,<sup>30</sup> while the current study was focused on cutting qualities of laser systems commonly used for surgical excisions. Potential comparison with these two wavelengths could be a scope of a future study.

The latest laser techniques of fiber lasers, which are now available for clinical use, emit in the IR region closely matching a local maximum of  $\mu_{a(\text{H}_2\text{O})}$ . In addition to its excellent beam quality, tissue interaction results in precise surgery, thus increasing its tissue safety.<sup>31</sup>

The handling of laser energy during tumor excision to obtain optimal cutting/coagulation effects is the cornerstone for any emerging LLPN technique. Generally, laser-tissue effects were dependent on a combination of adjustments (fiber velocity, distance to tissue and power output), which differed for each wavelength. Based on the presented results, surgeons can now pre-estimate laser-induced tissue effects. Intraoperative maneuvers could be optimized to the desired effect according to contact mode for cutting, distance for coagulation, the ablation threshold for each wavelength and the soft linear fiber velocity. From our clinical experience, a speed between 1 and 5 mm/s is favorable.<sup>5,32</sup> Fiber velocity of 10 mm/s was used to demonstrate the difference in tissue effects in comparison to the clinically applicable circumstances. This should encourage surgeons not to use rapid movements even in unexpected intra-operative problems (bleeding, etc.) when it became necessary to remove the tumor as fast as possible. These situations are not rare clinically. Surgeons, who are not aware of this, try always to avoid the use of LLPN as they fail to complete resections until the end with laser.

The coagulation zone could be considered as an indirect reflection or measure to haemostatic potential of lasers for the superficial parenchymal bleeding because 1. the needed control of diffuse superficial parenchymal bleeding (mini-vessels) is possible by a superficial layer of denatured tissue at surface. This will control it adequately. 2. The actual advantage of laser in tumor resections is the parallel cut/coagulation process. So the resulted depth of coagulation (in all directions) correlates with the laser capabilities of ablation in an area and coagulation in the depth and nearby surrounding tissue. This is of utmost importance clinically not only for coagulation but also to determine the lateral parenchymal loss. The control of bleeding vessels during resection requires directing the laser beam to the surrounding tissues and finally to the bleeding vessel itself in a circular or spiral manner.<sup>5,32</sup> In these situations, the laser energy would not offer a great advantage compared to other devices as the whole tissue response will depend on many factors, such as the diameter of the vessel, blood pressure inside it (artery or vein), normal blood coagulation, vessel position (central or if it retracted deeply in the tissues, etc.), etc., as well as laser adjustments (power, angle and duration of application, etc.). In clinical practice, a combination of instruments and sealants, or both, is generally utilized to obtain haemostasis. These multimodality efforts may be especially useful in case

of failure to control the renal bleeding intraoperatively. Lasers avoid the increase in the cost if multiple agents are employed. Combining suturing and haemostatic effects of laser may be the best strategy.

Some additional *in vivo* factors (variables) are of importance for the clinical setting and depend on the experience of the surgeon. Renal tumors are variable in position and its intra-renal depth, which necessitates continuous intraoperative change of fiber cutting angle to allow adequate resection. Another property of the kidney is its curved surface. While investigations on the influence of efficient sweeping angle dependencies are necessary as have been done for photoselective vaporization of the prostate,<sup>33</sup> adding this factor to the current experiments would have complicated the methodology without adding any clinically applicable advantage to the results (because of the above mentioned causes). Potentially, such an experiment could be performed in a separate study. So we constructed the current experiments with a perpendicular fiber tissues angle to mimic the clinical setting as surgeons will try to keep the fiber perpendicular to the cut plane in tissues as far as possible. Further, water rinsing is needed clinically to promote ablation without allowing superficial carbonization,<sup>32</sup> which was not necessary during the current experiments as the kidneys were not perfused and blood is already washed away. Using specially designed instruments that allow for parallel suction and water rinsing could improve further clinical LLPN studies.<sup>34</sup> Further, concentrating laser energy locally for coagulation of bleeding vessels completes haemostasis.

The NA of the fibers differs according to the used laser system. The bare fibers of wavelengths 940, 1320, and 1470 nm was NA = 0.37, while for 1064, 1940, and 2010 nm bare fibers had an NA = 0.2 as listed in Table 1. Using fibers of different core diameter (600  $\mu\text{m}$  versus 365  $\mu\text{m}$ ) in contact light application results in power irradiances (e.g., at 10 W: 3540 W/cm<sup>2</sup> versus 9560 W/cm<sup>2</sup>, respectively) in the contact area, which is far beyond the estimated tissue ablation threshold (about 250 W/cm<sup>2</sup>). Changing light application to a noncontact manner (5 mm distance), the difference in power irradiance of the two fiber diameters (600  $\mu\text{m}$  versus 365  $\mu\text{m}$ ) is reduced and is dependent on the NA of fiber. As an example at 10 W: 183 W/cm<sup>2</sup> versus 220 W/cm<sup>2</sup> at NA = 0.2, while 61 W/cm<sup>2</sup> versus 67 W/cm<sup>2</sup> at NA = 0.37, respectively. These values explain the observed good coagulation and reduced ablation in the experiments as shown in Fig. 6 when the distance between bare-fiber end and tissue surface is increased. While the effects of different fiber core diameters in contact mode remain nonsignificant as the example shown in Fig. 7. While the coagulation depth beyond the cut (ablation) area was proportionally deeper with increasing laser power (decreasing velocity) within limit, the superficial and axial depth was almost constant. This observation may be partly ascribed to the lowered conduction of heat from the carbonization layer that shields the penetration of light to deeper areas.

An illustration of cuts and its color changes are shown in Fig. 2(b) as well as the results demonstrated in Tables 3 and 4. All demonstrate the dynamics of carbonization in tissues. It should be pointed out that these clinically relevant results (optical judgement of laser effects) are just a subjective evaluation, which is susceptible to the restrictions and biases adherent to this art of evaluations like individual variations, the used high powers, the magnitude of increments of laser power,

etc. Further, high speed imaging of the ablation process, if available, would give a good impression of the mechanism of laser ablation.

The current results showed a significantly larger ablation depth when using the IR lasers compared to the NIR laser group (Fig. 4). Furthermore, the ablation threshold (ablation laser output power) seems lower for the IR laser group and a nonsignificant but shallower coagulation measurement was observed [Fig. 2(b)]. This could be explained by the dominated water absorption in the IR spectral region as confirmed by the wavelength dependency of the kidney tissue optical properties, shown in Fig. 8. The optical characters' measurements on renal tissues provide the rationale for the tissue effects. The use of a constant sample thickness of 200  $\mu\text{m}$  was thought to avoid any possible geometric disturbance in the concluded results. In addition the high absorption by IR lasers was accompanied with carbonization at low laser output powers, as mentioned in Table 3 and Fig. 2(b), which favoured the shielding of the light to penetrate into the depth of the tissue. This, in turn, results in a constant thickness of the heat conduction related coagulation layer in the lateral as well as in the axial direction.

Recently, several studies on feasibility and haemostatic potential of specific lasers for LLPN have been performed.<sup>5,27–29</sup> The current study reports on reproducible maneuvers, conditions and its outcome in terms of cutting quality as well as coagulation depth (as an indirect measure for haemostasis) for six different wavelengths, which is not available in literature so far. Additional testing of diverse laser-light emission modes, which could be selected in some laser systems (e.g., ON/OFF modes with constant duty cycle), showed no significant differences in all measured parameters compared to continuous mode at the same power outputs and experimental conditions (data not shown).

Current experiments were performed on fresh kidneys with intact renal capsule after removal of surrounding fat. Blood was also removed by rinsing, thus establishing reproducible (clinically mimicking) experimental conditions. Hemoglobin and blood are one of the main chromophore and absorber of tissue for light, when comparing the absorption spectra of hemoglobin and water.<sup>35</sup> In the current study, NIR and IR wavelengths are used as an energy source, thus the influence of tissue blood on the tissue absorption is reduced. According to previous experiences with the use of high laser powers in kidney vaporization experiments in underwater setup, perfusion of the organs with either heparinized blood or just saline solution resulted in a negligible difference in respect to macroscopic laser-tissue effects.<sup>30</sup> The potential difference of heat transport in the perfused *in vivo* kidney model (animal or human) should be the next scope of future evaluation studies.

Taking all previous considerations into account, as the physiology of tissue differs (e.g., human versus animal, *ex vivo* versus *in vivo*, nonperfused versus perfused), the local in-situ laser handling and maneuvers differ. Extrapolations from current experiments to clinical use require care. Successful *in vivo* LLPN technique based on current results was reported, which prove the clinical relevance of the current data.<sup>5,29,32</sup> Use of current wavelengths with described manipulations/maneuvers and knowledge of the basic interaction should contribute to decreased blood loss, maintain good oncological results (adequate tumor excision) and omitting or shortening renal ischemia during LLPN.

## 7 Conclusion

This *ex vivo* study shows that lasers are promising devices for both cutting and hemostatic procedures in LLPN/RPN. Their flexible transmission fibers are suitable for steerable laparoscopic instruments. As regards the induced tissue effects, application parameters (cutting velocity, fiber-tip tissue distance, fiber core diameter) are more important than the applied wavelength. All examined wavelengths were effective for RT resections.

## Acknowledgments

The authors would like to thank all companies mentioned in this work for their support and supplying their equipment. Thanks go also to K. Siegrist and M. Heide for the technical support.

## References

1. A. J. Pantuck, A. Zisman, and A. S. Beldegrun, "The changing natural history of renal cell carcinoma," *J. Urol.* **166**(5), 1611–1623 (2001).
2. D. A. Kunkle, B. L. Egleston, and R. G. Uzzo, "Excise, ablate or observe: the small renal mass dilemma: a meta-analysis and review," *J. Urol.* **179**(4), 1227–1233 (2008).
3. W. Jeong et al., "Laparoscopic partial nephrectomy versus robot-assisted laparoscopic partial nephrectomy," *J. Endourol.* **23**(9), 1457–1460 (2009).
4. B. R. Lane and I. S. Gill, "7-year oncological outcomes after laparoscopic and open partial nephrectomy," *J. Urol.* **183**(2), 473–479 (2010).
5. W. Y. Khoder et al., "The 1,318-nm diode laser supported partial nephrectomy in laparoscopic and open surgery: preliminary results of a prospective feasibility study," *Lasers Med. Sci.* **26**(5), 689–697 (2011).
6. L. P. Msezane et al., "Hemostatic agents and instruments in laparoscopic renal surgery," *J. Endourol.* **22**(3), 403–408 (2008).
7. Y. Lotan et al., "Clinical use of the holmium: YAG laser in laparoscopic partial nephrectomy," *J. Endourol.* **16**(5), 289–292 (2002).
8. Y. Lotan et al., "Laparoscopic partial nephrectomy using holmium laser in a porcine model," *J. Laparoendosc. Surg.* **8**(1), 51–55 (2004).
9. K. Ogan et al., "Laparoscopic partial nephrectomy with a diode laser: porcine results," *J. Endourol.* **16**(10), 749–753 (2002).
10. R. G. Hindley et al., "Laparoscopic partial nephrectomy using the potassium titanyl phosphate laser in a porcine model," *Urology* **67**(5), 1079–1083 (2006).
11. M. Liu et al., "Laparoscopic partial nephrectomy with saline-irrigated KTP laser in a porcine model," *J. Endourol.* **20**(12), 1096–1100 (2006).
12. T. M. Proebstle, T. Moehler, and S. Herdemann, "Reduced recanalization rates of the great saphenous vein after endovenous laser treatment with increased energy dosing: definition of a threshold for the endovenous fluence equivalent," *J. Vasc. Surg.* **44**(4), 834–839 (2006).
13. D. M. Wieliczka, S. Weng, and M. R. Querry, "Wedge shaped cell for highly absorbent liquids: infrared optical constants of water," *Appl. Opt.* **28**(9), 1714–1719 (1989).
14. K. F. Palmer and D. Williams, "Optical properties of water in the near infrared," *J. Opt. Soc. Am.* **64**(2), 1107–1110 (1974).
15. M. K. Louie et al., "Laparoscopic partial nephrectomy: six degrees of haemostasis," *BJU Int.* **107**(9), 1454–1459 (2011).
16. F. Porpiglia et al., "Laparoscopic versus open partial nephrectomy: analysis of current literature," *Eur. Urol.* **53**(4), 732–743 (2008).
17. R. H. Thompson et al., "Every minute counts when the renal hilum is clamped during partial nephrectomy," *Eur. Urol.* **58**(3), 340–345 (2010).
18. B. Turna et al., "Risk factor analysis of postoperative complications in laparoscopic partial nephrectomy," *J. Urol.* **179**(4), 1289–1295 (2008).
19. A. P. Ramani et al., "Complications of laparoscopic partial nephrectomy in 200 cases," *J. Urol.* **173**(1), 43–47 (2005).
20. T. Bach et al., "Laser treatment of benign prostatic obstruction: basics and physical differences," *Eur. Urol.* **61**(2), 317–325 (2012).
21. A. Breda et al., "Flexible ureteroscopy and laser lithotripsy for multiple unilateral intrarenal stones," *Eur. Urol.* **55**(5), 1190–1196 (2009).
22. S. A. Pierre and D. M. Albala, "The future of lasers in urology," *World J. Urol.* **25**(3), 275–283 (2007).

23. V. Eret et al., "GreenLight (532 nm) laser partial nephrectomy followed by suturing of collecting system without renal hilar clamping in porcine model," *Urology* **73**(5), 1115–1118 (2009).
24. M. H. Bui et al., "Less smoke and minimal tissue carbonization using a thulium laser for laparoscopic partial nephrectomy without hilar clamping in a porcine model," *J. Endourol.* **21**(9), 1107–1111 (2007).
25. J. K. Anderson et al., "Large-volume laparoscopic partial nephrectomy using the potassium-titanyl-phosphate (KTP) laser in a survival porcine model," *Eur. Urol.* **51**(3), 749–754 (2007).
26. D. D. Theisen-Kunde et al., "Comparison between a 1.92- $\mu$ m fiber laser and a standard HF-dissection device for nephron-sparing kidney resection in a porcine in vivo study," *Lasers Med Sci.* **26**(4), 509–514 (2011).
27. S. Mattioli et al., "What does Revolix laser contribute to partial nephrectomy," *Arch. Esp. Urol.* **61**(9), 1126–1129 (2008).
28. T. Gruschwitz et al., "Laser-supported partial nephrectomy for renal cell carcinoma," *Urology* **71**(2), 334–336 (2008).
29. W. Y. Khoder et al., "Outcome of laser assisted laparoscopic partial nephrectomy without ischemia for peripheral renal tumours," *World J. Urol.* (2011) (Epub ahead of print).
30. M. Seitz et al., "High-power diode laser at 980 nm for the treatment of benign prostatic hyperplasia: ex vivo investigations on porcine kidneys and human cadaver prostates," *Lasers Med. Sci.* **24**(2), 172–178 (2009).
31. A. J. Marks and Joel M. H. Teichman, "Lasers in clinical urology: state of the art and new horizons," *World J. Urol.* **25**(3), 227–233 (2007).
32. W. Y. Khoder et al., "Laser-assisted laparoscopic partial nephrectomy without ischemia: procedure and challenges," *J. Endourol. Part B Videourology* (2011).
33. W. J. Ko et al., "Defining optimal laser-fiber sweeping angle for effective tissue vaporization using 180 W 532 nm lithium triborate laser," *J. Endourol.* **26**(4), 313–317 (2012).
34. W. Y. Khoder and R. Sroka, "Concept of a fiber guidance instrument for laser-assisted laparoscopic partial nephrectomy," *Med. Laser Appl.* **26**(4), 176–182 (2011).
35. S. Prahl, "Optical absorption of haemoglobin and water," Oregon Medical Laser Center, <http://omlc.ogi.edu/spectra/> (2001).